Hittite Journal of Science and Engineering, 2022, 9 (4) 241–251
ISSN NUMBER: 2148–4171
DOI: 10.17350/HJSE19030000277

EEG-induced Fear-type Emotion Classification Through Wavelet Packet Decomposition, Wavelet Entropy, and SVM

Caglar Uyulan[1] **Ahmet Ergun Gumus**[2] **Zozan Guleken**[3]
[1]Izmir Katip Celebi University, Department of Mechanical Engineering, Izmir, Turkey
[2]Uskudar University, Department of Neuroscience, Istanbul, Turkey
[3]Uskudar University, Department of Physiology, Istanbul, Turkey

Article History:
Received: 2022/03/03
Accepted: 2022/12/19
Online: 2022/12/31

Correspondence to:*Zozan Guleken*
Department of Physiology, Uskudar University, 34400 İstanbul, Turkey
Tel: +90 533 604 1726
E-Mail:zozan.guleken@uskudar.edu.tr

ABSTRACT

Among the most significant characteristics of human beings is their ability to feel emotions. In recent years, human-machine interface (HM) research has centred on ways to empower the classification of emotions. Mainly, human-computer interaction (HCI) research concentrates on methods that enable computers to reveal the emotional states of humans. This research proposed an emotion detection system based on visual IAPPS pictures through EMOTIV EPOC EEG signals. We employed EEG signals acquired from channels (AF3, F7, F3, FC5, T7, P7, O1, O2, P8, T8, FC6, F4, F8, AF4) for individuals in a visually induced setting (IAPS fear and neutral aroused pictures). The wavelet packet transform (WPT) combined with the wavelet entropy algorithm was applied to the EEG signals. The entropy values were extracted for every two classes. Finally, these feature matrices were fed into the SVM (Support Vector Machine) type classifier to generate the classification model. Also, we evaluated the proposed algorithm as an area under the ROC (Receiver Operating Characteristic) curve, or simply AUC (Area under the curve) was utilised as an alternative single-number measure. Overall classification accuracy was obtained at 91.0%. For classification, the AUC value given for SVM was 0.97. The calculations confirmed that the proposed approaches successfully detect the emotion of fear stimuli via EMOTIV EPOC EEG signals and that the classification accuracy is acceptable.

Keywords:
EMOTIV EPOC EEG; Fear emotion; Wavelet Entropy; SVM; ROC.

INTRODUCTION

Even though the human emotional experience is essential in our daily lives, our scientific understan-ding of human emotions is still quite restricted. The advancement of the affective science field is critical for the advancement of psychology for societal detri-ments and solicitations. Identifying emotional signals in ordinary life is becoming increasingly significant as it affects people's communication through verbal and nonverbal actions [1]. Especially for people who have communication difficulties, it is crucial to determine their emotions correctly. Various methods are being developed to monitor the physiological effects of emotions with technological tools. Among these methods, there exist various medical imaging techniques.

Along with devices, i.e. fMRI, EEG, GSR, and Faci-al Coding that allows emotions to be monitored, much work is being done on newly developed computational methods. EEG devices, which are among these devices, enable analysis by recording brain waves with high temporal resolution. Emotions are tried to be revealed by using machine learning (ML) methods on brain waves recorded with EEG. Studies are carried out to identify emotions online or offline. Face expressions are one example of emotional signals, which are believed to be one of the most instant ways humans express their feelings and intentions [2]. With advancements in brain-computer interface (BCI) and neuroimaging technology, it becomes possible to use a portable EEG headset to acquire brainwave signals non-intrusively and measure or control the motions of devices virtually [3]. When machines are incorporated into the system to assist in recognising these emotions, it enhances efficiency and lowers costs in several ways [4]. With the development of technology and population reduction, there is a significant interest in understanding emotional interactions, and reliable and feasible methods are needed to identify human emotional states [5]. Individual understandings may reveal a person's emotional condition. Self-Assessment Manikin (SAM) [6] is utilised to evaluate a state of mind as a self-evaluation [7], that is, visually presented pleasure-displeasure images, degree of arousal, and dominance-submissiveness. People's emotional experiences throughout their lives are neurobiological activities of the human brain. We can investigate a person's emotional responses when exposed to certain situations by directly accessing their electroencephalogram (EEG) signals. This evidence from brainwave signals can be used to enhance and verify whether or not a person is substantially healthy or have a mental disease [8]. EEG headset comes in a variety of design concepts and costs. The distinction is that the sort of electrodes used to capture the brainwave data has an impact on both the quality and duration of the setup [9]. The electrode numbers are put over the human scalp, and the EEG headset resolution varies concerning design quality-related accessibility [10]. The design of the EEG headsets may differ, such as the 14-channel Emotiv EPOC+, and electrodeposition may address the temporal, parietal, and occipital lobes. These EEG headsets include wireless data transmission features, so no long wires are trailing around the body, making this equipment portable and simple to set up [11]. Artefacts are signals collected by the electrodes due to muscular activity [12].

Additionally, external interferences such as auditory noise or sensation may induce distortions in the EEG during collection, which must be eliminated using filtering algorithms [13]. Finally, to assess EEG signals for emotion classification with ML algorithms, the brainwave signals must be represented in the frequency domain through a fast Fourier transform (FFT) [14]. Recent studies were published with Emotiv EPOC+ headsets to obtain several types of brainwave recordings and determined frequency bands [15]. Artificial intelligence and ML are currently being dynamically settled and researched to adapt to intuitive approaches. Neuroinformatics is a science that examines emotion classification by collecting EEG signals and classifying them with ML algorithms. This would aid in improving human-computer interactions to meet human requirements [16]. Emotion evaluation leads to emotion integration into human-machine interaction (HCI) systems. Over the last few years, many studies have assessed emotion and stress. Different emotion detection systems based on brain signals [17] and the application of entropy in bio-signal processing have already been addressed in other relevant works [18]. Fear is less common among the emotions trying to be determined with EEG devices.

Related Works

In [19] [62], an efficient spatial feature extraction and feature selection method having a short processing time was proposed to classify human emotions. The Spatio-temporal analysis was performed using complex continuous wavelet transform to collect whole time-frequency information. Then, three different Deep Neural Networks were utilised to obtain a combined feature vector. In [20] [63], a hybrid of manual and automatic feature extraction methods has been proposed. The asymmetry in various brain regions is collected in a 2D vector named AsMap from the differential entropy features of EEG signals. A thorough comparison was conducted with other feature extraction methods, and a convolutional neural network model was used in the classification process. The emotion EEG dataset reached the highest classification accuracy of 97.10%. An EEG emotion classification network based on attention fusing was proposed in [21] [64]. The multi-channel band features were extracted and then fused using attention units. The algorithm's performance was verified on an open-access dataset SEED and the self-collected dataset LE-EEG. The proposed model applying five-fold cross-validation obtained the highest accuracy of 96.45%.

[22] [65] developed the EEG signals-based automated cross-subject emotion recognition framework that exhibits good generalizability and high classification accuracy of cross-subjects using the Fourier-Bessel series expansion-based empirical wavelet transform method. The training and testing of the models were performed using 10-fold cross-validation by training the feature vectors via ensemble bagged tree classifiers.

A deep convolutional neural network model for emotion classification utilising a non-end-to-end training method was proposed in [23] [66]. The proposed model achieved a high accuracy of 93.7%, and the extracted features exhibited the best separability among the tested models, proved with the feature visualisation technique. A novel multi-feature fusion network with spatial and temporal neural network structures was developed in [24] [67] to learn discriminative Spatiotemporal emotional information. Two common types of features, time-domain features (Hjorth, Differential Entropy, Sample Entropy) and frequency domain features (Power Spectral Density), were extracted. The experimental results on the DEAP dataset showed an average emotion recognition accuracy of 80.52%.

In [25] [68], three deep learning-based models (RNN, LSTM, and GRU) were compared for emotion recognition using EEG signals. The efficiency of these networks was validated by experimental data using the EEG Brain Wave Dataset.

[26] [69] proposes a novel four-stage method for human emotion recognition using multivariate EEG signals.

These methods are multivariate variational mode decomposition, joint instantaneous frequency and amplitude, and deep residual convolutional neural network ResNet-18, respectively. The experimental results show the best accuracy of 99.03%, 97.59%, and 97.755% percent for classifying arousal, dominance, and valence emotions, respectively. In [27] [70], a method for capturing the distinct minimum spanning tree topology that underpins the different emotions was developed. A hierarchical aggregation-based graph neural network was used to investigate the MST structure in emotion recognition.

In light of recent studies, we proposed to evaluate possible signal changes in brain waves during fear stimuli through the EMOTIV EPOC EEG device. This study aims to classify the emotion of fear using the wavelet technique using the Emotiv EPOC EEG device. Then after the data acquisition procedure, the features retrieved from the entropy parameters and the classification methods were used to discriminate fear and neural emotions.

MATERIAL AND METHODS

Experimental Design and Data Acquisition

Before the simulations, participants were asked to complete a questionnaire regarding the selected IAPS [International Affective Picture System] picture. Because it is likely that the emotion a participant experience was not the same as what was imagined. As a result, the subject is asked to review his feeling on a self-administered scale. Then, Among the IAPS photographs, fear-related and neutral pictures that were highly scored were chosen as a fear stimulus to provide a somatosensory stimulation in this study protocol. 1050, 1120, 1200, 1201, 1270, 1274, 1280, 1300, 1302, 1930, 1931, 2770, 2811, 3001, 3061, 6021, 6313, 6315, 6370, 6510, 8160, 8480, 9000, 9050, 9440, 9584, 9590, 9600, for neutral stimuli with the number; 5621, 5629, 5001, 5300, 5410, 5594, 5600, 5814, 7175, 7235 were used in random order, but in the same order for each participant. IAPS designated various fear stimuli, Center for the Study of Emotion and Attention [28] was shown to the attendees as a stimulus set in the front of the computer screen to assess the responses to the fear and neutral stimulus with the EMOTIV EPOC EEG device. Participants completed the SAM-Self-Assessment Manikin questions regarding the stimuli after each photo zoomed on the screen for 3 seconds. The SAM form is used to evaluate the subjects' emotional state in response to a stimulus. In emotion research, self-evaluation measures are usually employed to analyse emotions. Arousal, valence, and dominance criteria have been used to analyse emotions [29]. The subjects wore an EMOTIV EPOC EEG device for the duration of the experiment, which was videotaped. Schematics of EMOTIV EPOC data acquisition are shown in Figure 1a, and the Epoc + channels localisation covered in the analysis according to the 10–20 system is shown in Figure 1b. None of the participants had neurological symptoms, and all had healthy or normal vision. All of the participants signed the document written consent form. All participants were aware of the process and were not paid for their support. Experiments were approved by the human subject board of Uskudar University's Ethics Committee in Turkey (14-02-20212 with 61351342 number decisions) under the ethical principles outlined in the 1964 Declaration of Helsinki (World Medical Organization, 1996).

EMOTIV EPOC EEG recordings and Preprocessing

The recording of emotional data is the initial step toward emotion recognition. Every standard test for assessing emotion and stress states has benefits and drawbacks [28]. Most studies that use EEG signals to detect emotion utilise images from the International Affective Picture System (IAPS). Several American participants rated the IAPS on two dimensions of nine points each (1-9). IAPS usage allows for more precise regulation of emotional stimuli as well as a more straightforward experimental design [30]. We picked the visual presentation test for this study since its assessment was closest to our objectives. Some photographs were used as stimuli to evoke the intended emotions (neutral and fear-stimulated). The EEG equipment EMOTIVTM used in the experiment is a portable, practical and inexpensive model compared to the clinical EEG devices of the EMOTIV brand, as seen in Fig. 1a. EEG signals were collected during emotional sessions at Uskudar University Istanbul, Turkey. This headset EMOTIVTM (version 2015) is composed of 14 usable saline electrodes positioned according to the 10/20 system (AF3, F7, F3, FC5, T7, P7, O1, O2, P8, T8, FC6, F4, F8, AF4) Fig. 1b and two references on parietal sites (P3 and P4) CMS / DRL references right and left mastoids.

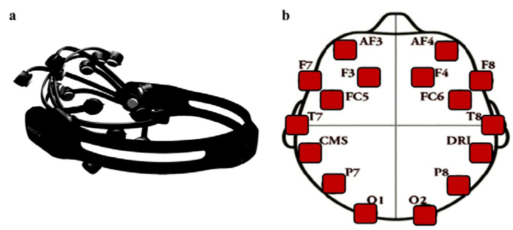

Figure 1. (a) Schematics of EMOTIVTM EPOC EEG headset (b) Positioning of the Epoc + channels included in the analysis over the scalp according to the 10–20 system. Source: https://www.emotiv.com/.

Low-energy Bluetooth provides a wireless computer connection. The USB receiver transmits data over 2.4 GHz. For more detail, one can investigate the technical specifications at the following link: https://emotiv.gitbook.io/epoc-user-manual/ 15 volunteers, eight women and seven men, participated in the experiment. The mean age of these subjects was 44, and the standard deviation of the ages was 11.8. Attention was paid to ensuring that the subjects did not have any inconvenience regarding using EEG. This study recorded EEG data with the Test Bench program and synchronised it with an open-source Open Sesame program (version 3.3.8). A virtual serial port was installed on the computer to synchronise the EEG records with the IAPS pictures presented on the screen. A Python software (version 3.8.7) script was written that runs inside the Open Sesame program to provide synchronised data flow to the input and output channels of the virtual serial port. Thus, as soon as the pictures were on the screen, the Open Sesame program sent a trigger to the Test Bench program via a virtual serial port. Synchronisation is achieved on the same computer with a virtual port. Impedance was controlled at the initialisation of the recording via the Test Bench program. We used the EEGLAB Software program (version 2021.0) to pre-process all the EEG data, which is an open-source program and runs on MATLAB© (version R2020b) as used in previous studies [31]. All processing code is available at Open Science Framework (https://sccn.ucsd.edu/eeglab/download.php). After the pre-processing process, EEG data was saved in the Testbench program as a ".edf" extension. Then, these files were transferred to the EEGLAB program, and channel information and electrode location information were obtained from the data file. Signals were filtered between 0.2-45 Hz with the Basic FIR band-pass filter and 1- Hz Basic FIR high-pass filter method as an artefact removal process.

Afterward, epochs in the range of 100-1000 ms were determined to evaluate the responses to the stimuli. Independent component analysis (ICA) was performed [32]. Following filtering, all epochs were visually scanned, and artefacts caused by motor, visual or muscular movements were rejected in the pre-processing stage of the EEGLAB Software program. After the pre-processing stage, the analysis part was started on EEGLAB. To determine the differences between two levels of emotion, Fear and Neutral stimuli, EEG data was divided into two sub-data files, Fear and Neutral. In these data files, only the EEG recordings of the relevant pictures were included in the analyses. After topographic interpolating the rejected channels, the clean data were saved by separating fear and neutral epochs into two files for each subject.

Feature Extraction and Classification; The Wavelet Packet Transform and Wavelet Entropy

The data analysis having multiple levels of scale is realised through the Wavelet Transform (WT) by preserving the transient events in the data. Wavelet is an oscillatory window function having a distinct shape and zero mean value. Since CWT is computationally expensive and produces redundant information, DWT with sub-band coding should be used for efficiency concerns. The two-dimensional time-scale domain is formed due to the implementation of the WT to the time-series data. In WT, the entire signal is examined through various-sized windows. The size of the windows depends on the frequency characteristics in the parts of the signal. Small windows are used in the high-frequency parts for increasing time resolution, while more oversized windows are applied to capture important frequency information in the low-frequency parts.

Wavelet Packet Transform (WPT) has a generalisation ability for the time-frequency analysis of the WT. In the WPT, the data is fed to the scaling and wavelet filters (low-pass and high-pass filters having complementary bandwidths), whose outputs are downsampled by a factor of two by applying a convolution operation. The outputs of the high-pass filtered data correspond to the detail coefficients, and the outputs of the low-pass filtered data match the approximation coefficients at that scale level. The approximation coefficients are utilised as the sampled data input subject to the next pair of wavelet filters. This sequential process continues until the unit interval limit is converged. However, the wavelet transform operation can be terminated at any level. If the transform has n level, the minimum length limit of the data set would be2^n. The schematic flowchart of the WPT algorithm can be seen in Fig. 2.

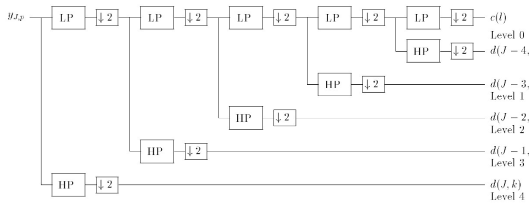

Figure 2. The partial graph of a binary tree of the WPT algorithm. (J is the transformation level).

The multi-rate filter bank comprises a series of half-band high-pass and low-pass FIR filters and decimators; however, the WPT is a more flexible method than subband coding because it separates the signal into a well-suited subband signal. The wavelet filters are constructed to be orthonormal transform kernels. The set of detail and approximation coefficients at each level of decomposition corresponds to a subspace pair that WT creates. These subspaces cover frequency subbands of the original data set. Any set of disjoint subspaces is on an orthonormal basis having different subband intervals. The transform coefficients evaluated at each level correlate with the original data set and are waveform functions (Symlet, Daubechies, etc.) demonstrating the wavelet packet. Such decomposition is achieved by shifting and scaling the chosen wavelet function and projecting the signal on the subspace. Various bases of the WPT can be utilised as arbitrary adaptive tree-structured filter banks.

The best orthonormal basis can be chosen through a search algorithm (i.e. Pruning, Growth), which minimises the information cost function measuring signal energy distribution, such as Shannon entropy, Log Energy, Coifman-Wickerhauser entropy, etc. [33].

WPT generalises the WT and provides a more flexible tool to analyse the time-frequency features of the data [25, 26, 27]. The most crucial time-frequency features are extracted by reducing the computational cost and avoiding redundancy.

One can define the connection between wavelets and filters by first describing the wavelet transform as in Equation 1

$$\psi_f(a,t) = \frac{1}{\sqrt{a}} \int_{-\infty}^{+\infty} f(\tau) h^*\left(\frac{\tau - t}{a}\right) d\tau \tag{1}$$

Where a is the scale parameter, t is the shift parameter which indicates the centre location of the window as it is shifted through the signal, the variable τ is denoted as time, $f(.)$ is the original signal or data in the time-domain, $h^*(.)$ refers to the wavelet basis.

While high-scale values support a broad view of the signal, as a controversy, low-scale values will pick up the detail of the signal.

Then, Equation1 can be rewritten as in Equation 2

$$\psi_f(a,t) = f(t) \otimes h_a^*(t) = f(t) * h_a^*(-t) \tag{2}$$

The symbol $\otimes$ represents the correlation operation, and the symbol indicates the convolution operation.

Since the wavelet family $h_{j,k}(t)$ is an orthonormal basis , $L^2(\Re)$ the energy-like function is derived from the wavelet coefficients as given in Equation 3

$$T_j = \sum_k \left|\psi_j(k)\right|^2 \tag{3}$$

where the subscript $j = -1, \ldots, -N$ indicates the resolution level.

The energy at each sampled time will be like in Equation 4

$$T_j(k) = \sum_{j=-N}^{-1} \left|\psi_j(k)\right|^2 \tag{4}$$

The total energy can be represented in Equation 5

$$T_{total} = \sum_{j \prec 0} \sum_k \left|\psi_j(k)\right|^2 \tag{5}$$

Then, the normalised values, which give the relative wavelet energy, are stated as in Equation 6

$$p_j = \frac{T_j}{T_{total}} \tag{6}$$

Equation 6 defines the probability distribution of the energy for each resolution level.

This identity gives a flexible tool to identify specific phenomena in the time-frequency plane. The energy term is obtained for the usage in the derivation of the wavelet entropy (WE) equation.

According to the Shannon entropy [37], the information of the wavelet energy distribution is defined in Equation 7

$$S_\psi(p) = -\sum_{j \prec 0} p_j \ln\left[p_j\right] \tag{7}$$

S_ψ is stated as total WE, a degree of order/disorder measure of the signal. We reveal the hidden process related to the original signal. It can be predicted that an ordered signal behaves like a periodic mono-frequency signal having a narrowband spectrum. A wavelet representation of this kind of signal is encoded in one individual wavelet resolution level. Therefore all relative wavelet energies are almost zero except for the individual level. In contrast, a random signal demonstrates very disordered behaviour. This means that all frequency bands are equally contributed. Therefore the relative wavelet energy is almost the same for all resolution levels, and the WE takes maximum values [38].

Support Vector Machine

Some methods, i.e. perceptron, find a separating suboptimal hyperplane considering some criterion of expected goodness. Support Vector Machine [SVM] searches for an optimal solution while maximising the margin between classes in a high dimensional feature space around the separating hyperplane. A subcategory training of the samples characterises the decision function. SVM can perform classification utilising the support vectors rather than the entire dataset, and therefore it is robust to outliers and make very efficient predictions [39].

Methodology

The feature extraction methodology proposed in this paper was inspired by the combination of the methods used in the papers [31, 18,32]. After pre-processing steps, we obtain two data matrices corresponding to control and fear-type emotion-driven groups, each of which has 14592 samples for every 15 electrodes. Then, the WPT was applied to each group of data. The multiscale WPT feature extraction code used in this paper was adapted from [33-34]. Since acquired EEG signals were sampled at 128 Hz, the number of samples per window we extract features were selected as 128, and spacing of the windows or simply the increments among windows was selected as 16. The decomposition level is 7. 255 features for every 15 electrodes were extracted for a complete tree at this level. Therefore, the WPT feature matrix size is [905,3825 [255*15]]. Afterwards, wavelet entropies were evaluated from the WPT feature matrix to reduce the data size and obtain a robust biomarker for the classification. At this stage, the feature matrix was separated into fractions, that each fraction has 255 samples for every 15 electrodes. The size of each fractioned matrix is [905,255]. The number of the total fractioned matrices is 15, which corresponds to the electrode number. The wavelet entropy code used in this paper was adopted from [38]. The wavelet filter was selected as "Coiflet-4" and the decomposition level was chosen as 4 after making a comparative analysis, which shares the same procedure stated in [44]. Coiflets performed relatively better compared to other wavelet families. When the wavelet entropy algorithm was applied to these matrices, [255,15]-sized feature matrix, which contains the entropy values, were acquired for every two classes. Finally, these feature matrices were fed into the SVM-type classifier to generate the classification model. The flowchart of the proposed methodology is demonstrated in Fig. 3.

The classification was done via the Classification Learner app in the Matlab environment. The Classification Learner app trains models for the classification process. By utilising this app, it is possible to generate supervised ML models. It is a flexible and automated tool to search for the best classification model type, i.e. decision tree, SVMs, nearest neighbours, ensemble methods, etc. The data, including two classes (fear-type induced and control) and their labels, were trained, and a classification model that generates a prediction for the response to new data was built.

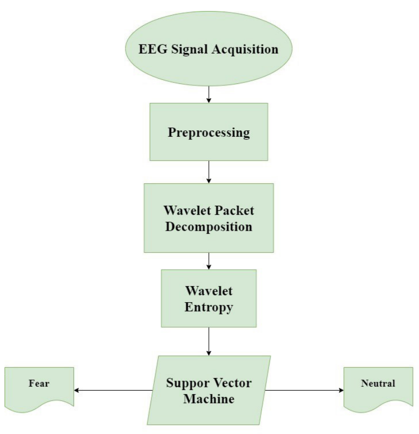

Figure 3. Flowchart of the signal processing methodology.

RESULTS

Classification Results using SVM Kernels

Control and fear-type emotion-driven groups were classified using an optimisable SVM model.

Training involves the minimisation of the error function as given in Equation 8.

$$min_{w,b,\xi}\left[\frac{1}{2}W^TW + C\sum_{i=1}^{l}\xi_i\right] \tag{8}$$

The error function is subjected to the constraints: $y_i\left(W^T\varphi(x_i)+b\right)\geq\xi_i and\ \xi_i\geq 0, i=1,\ldots l$. Here $X_i \in R^n, i=1,\ldots l$ are training data in vector form showing the classes, and $y\in R^l$. It is a vector such that $y_i\in\{1,-1\}$, W is the coefficient vector, b is a constant and ξ_i are parameters that handle non-separable inputs. Support vectors are used to define the dual error and the decision function [45].

The hyperparameters of the SVM model were optimised. The hyperparameter search range is listed as box constraint level: 0.001-1000, kernel scale: 0.001-1000, kernel functions: Gaussian, Linear, Quadratic, and Cubic, and standardised data: accurate. The optimiser option was selected as Bayesian optimisation; the acquisition function was "expected improvement per second plus" with 30 iterations. All features are used in the model, and Principle Component Analysis is disabled. After the optimisation process, the minimum classification error was obtained with the cubic kernel whose scale is one, whose box constraint level is 15.1782. The minimum classification error plot is given in Fig. 4.

The following information was included in the minimum classification error plot. Estimated minimum classification error corresponds to a minimum classification error estimation evaluated through optimisation conducted with the trial sets of hyperparameter values. The best point hyperparameters description refers to the estimate corresponding to an upper confidence interval evaluated from the objective model of classification error. The optimised hyperparameters do not guarantee the observed minimum classification error. The Bayesian optimisation algorithm selects the set of hyperparameter values that minimises an upper confidence interval for the objective model built to evaluate the classification error. The minimum error hyperparameters indicate the iteration corresponding to the hyperparameters that yield the observed minimum classifi-

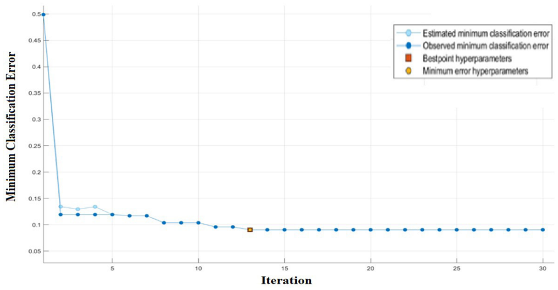

Figure 4. The minimum classification error plot.

cation error. If the grid search was used to perform hyperparameter optimisation, the best point hyperparameters and the minimum error hyperparameters are identical. 10-fold cross-validation was used in the training and testing of the classifier. The optimised SVM classifier's classification result is given in Table 1. The number of true positive (TP), false-negative (FN), true negative (TN), and false-positive (FP) subjects and accuracies are also considered to calculate the classifier performance. The results represent the mean values after a 10-fold CV for the robustness of the classification performance.

The classification results are given in Fig. 5. The figure illustrates the spectral SVM classification results.

Also, to evaluate the proposed algorithm, the area under the ROC (Receiver Operating Characteristics) curve is utilised as a measure represented by a single number. Overall accuracy was obtained at 90.98%.

Table 1. Confusion matrix and the other classification metrics.

	Actual Values	
Predicted Values	*235*	*20*
	26	*229*
Recall/Sensitivity [TPR]	*0.900383142*	
Precision	*0.921568627*	
Specificity [TNR]	*0.919678715*	
Overall Accuracy	*0.909803922*	
F-Measure	*0.910852713*	

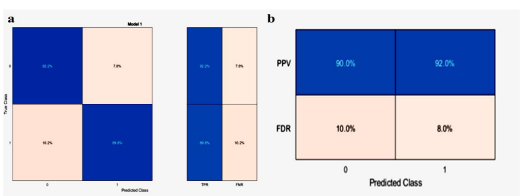

Figure 5. According to the best classification results of the confusion matrix for fear and neutral stimuli conditions. (a) illustrates confusion matrix as a percentile (b) is the results of positive predictive value and false discovery rate shown.

The SVM-based optimised classifier reached 90.03% sensitivity, 92.15% precision, 91.96%, and 91.08% F-measure, respectively. The external validation was conducted to estimate the generalisation method using different data. New data comprising 20 subjects (10 neutral/10 fear-type induced) were processed through the same methodology to achieve external validation criteria. SVM-based classifier performed 93.6% classification sensitivity, and 85.45% and 88.54% classification sensitivity was achieved by Naive Bayes (NB) and kNN-based classifiers, respectively. ANN classifier reached 89.78% classification sensitivity. The classification results of the classifiers with external validation are tabulated in Table 2. For classification, the AUC value is given in Fig. 6 for SVM as 0.97.

Table 2. The classification results of the classifier with external validation. (Abbreviations; SVM: Support Vector Machine, NB: Naive Bayesian, k-NN: k-Nearest Neighbor, ANN: Artificial Neural Network).

Classifier	*Sensitivity [%]*	*Precision [%]*	*Specificity [%]*	*F-measure [%]*	*Accuracy [%]*
SVM	*93.6*	*92.88*	*92.71*	*93.25*	*93.17*
NB	*85.45*	*87.03*	*86.74*	*86.23*	*86.08*
k-NN	*88.54*	*87.93*	*86.79*	*88.23*	*87.71*
ANN	*89.78*	*89.23*	*86.79*	*89.50*	*88.43*

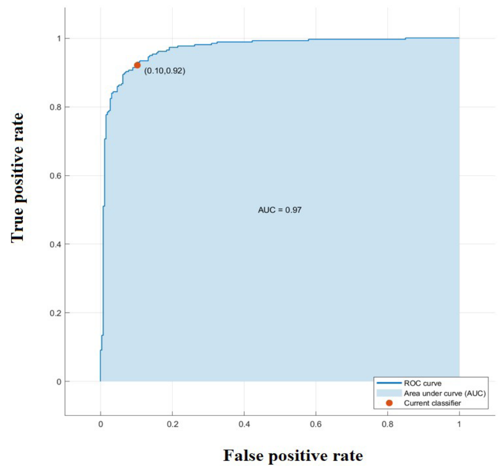

Figure 6. The results of the features excluded from the EMOTIV EPOC EEG signals by ROC Curve of Classification Method. (AUC: Area Under the Curve)

ROC analysis has been used in many scientific fields in which a graphical representation is needed, such as radiology, medicine, deep learning, bioinformatics, etc. Area Under Curve (AUC), derived from ROC analysis, is a key metric for interpreting the classification models. The classification models can be trained by considering cost proportion and distribution of the class in the operating condition, and then they are transferred to a different operating condition. ROC is a space decomposition that infers the performance of the classification model in a dual-comparative manner. The x-axis represents the false positive rate (FPR), and the y-axis is responsible for the valid positive rate (TPR). The visualisation of the TPR and FPR changes can be described in the ROC curve, and also the evolution can be seen for the same classifier for a threshold range. Soft classifiers adapt to an operating condition. Besides, ROC analysis illustrates how the performance of the classification models and threshold confidence are evaluated [46]. A comparative study that focuses on different methods for the performance of classifications was done based on the employment of the ROC-AUC score utilised for ML applications [47].

DISCUSSION

Facial emotions were widely used for emotion recognition; however, this method is not preferred for classification because conducting an unbiased experiment is impossible. The experiments conducted through EEG devices are more reliable, efficient, and robust, giving unbiased classification performance data. Systematic reviews were conducted thoroughly for EEG signal-based emotion classification, feature extraction, brain condition, group comparison, etc. [48].

Since EEG signals have a non-stationary nature, the transformations in the frequency domain are inadequate, so one should consider the time domain information associated with the frequency domain. WPT/DWT-based feature extraction methods are quite effective in analysing the EEG signals by extracting time-frequency information simultaneously for developing an emotion recognition system [49] because this method serves as a multi-resolution solution, which overcomes the signal resolution problem that originated from Heisenberg's uncertainty principle. The efficiency of the classification for various kinds of WT can be compared, and the best wavelet transform method is found [50]. The raw EEG signals obtained by audio-visual stimuli-based protocol evoking the discrete emotions were preprocessed by the Surface Laplacian filtering approach and partitioned into five prominent bands of brainwave using WT having various wavelet functions. The validation was done using 5-fold CV, and the classifier was proposed as kNN-k Nearest Neighbor, which has given a maximum average classification rate of 82.87% on 62 channels, and 91.33% on the beta band with short-time FFT [14, 42] was found emotional state classification accuracy of 86.75% for arousal level and 84.05% for valence level, by applying SVM and kNN. Especially the gamma band yielded higher accuracy than low-frequency bands of EEG signal. The effectiveness of utilising a time-frequency component combination and DWT feature for emotion recognition was studied through the IAP and EEG response images. The maximum classification accuracy was obtained via ANN as 81.88% [52].

Moreover, DWT coefficients having different wavelet functions, i.e. coiflets, Daubechies, and symlets, were used with Extreme Learning Machine and SVM for improving the emotion recognition performance [53] used adaptive WP Filter-Bank for speech emotion recognition. Besides WT, the entropy-related features have significantly succeeded in EEE-based emotion recognition [54]. A comparative classification methodology was employed with an SVM, MLP, and 1D-CNN combined with features extracted from six entropy measures [55]. A PSD-based emotion state classification was done in [56] by stating two simple decision rules to classify positive and negative emotions. The four emotion states, joy, relaxation, sadness, and fear, were classified through kNN, multilayer perceptron, and SVM. The experimental results revealed that the frontal and parietal EEG signals were more informative about emotional states. The average test accuracy for this kind of multi-class classifier was obtained as 66.51% [57]. In another study [58], the mean and standard deviation of Euclidean distances are computed from a 3-D phase space diagram. These features have fed into the multi-class least squares SVM with Morlet wavelet kernel function to discriminate four emotions. After 10-k CV, they found 91.04% accuracy. In the paper [59], EEG-based emotion recognition was developed through Shannon entropy, cross-correlation and autoregressive modelling. The emotions, i.e., happiness, sadness, hatred, were classified using Multi-Class SVM with an accuracy of 94.097%. In the paper [60], a new method to recognise emotion from raw EEG signals by using LSTM-RNN was proposed and the proposed algorithm, which gives an average accuracy of 85.65%, 85.45%, and 87.99% with arousal, valence, and liking classes, respectively, was verified through the DEAP dataset. Emotion classifications were also performed through Naive Bayesian, Autoregressive model, ANFIS etc. [61]. Recently, deep learning-based methods, i.e. CNN, LSTM, GRU, SAE have also been used for emotion recognition [62].

The experimental results showed that conditional transfer learning methodology enhances emotion valence and arousal classification performance [63]. It was proven that to improve emotion recognition combining, feature selection and kernel classifiers can be combined [64]. A novel deep learning-based method using CNNs for EEG-based emotion recognition was employed, including brain connectivity features [65]. In the paper [66], functional connectivity matrices and CNN was employed to classify several emotional tasks. The model with a 4-classification task demonstrated 75% average accuracy. [67], applied a four-class emotion classification method, SVM and kNN combined with Hjorth parameters. The fractal dimension feature was extracted and classified using SVM with radial basis function in [68]. In the paper [69]. ICA combined with SVM was found to recognise happy and sad emotions with an accuracy of 87.5% and 92.5%. The LIBSVM model classified two emotional dimensions of Arousal and Valance with a 74.88% and 82.63% average recognition rate [70].

LIMITATIONS

The suitability of IAPS pictures for Turkish culture and heritage is questionable. To induce fear emotions, additional non-IAPS pictures would have been utilised. The EEG device used in data acquisition had only 14 channels. The additional usage of a clinically approved multi-channel device would have allowed verifying the results. The number of participants was 15 in our study; the number was limited due to Covid 19 disease.

CONCLUSION

This research was conducted to reveal the effect of fear-type emotion after stimuli and to find an efficient classification feature in identifying this effect from the EEG signals. We utilised the potential of localising the frequency bands in EEG signals through WPT and fusing through Wavelet entropy to obtain efficient features utilised in the classification. The classification method was also optimised. The results can be compared well with other ML techniques, i.e. learning vector quantisation, k-nearest neighbours, and multilayer perceptron. Electrode selection through the feature selection process might enhance the recognition rate and produce better results.

In conclusion, WPT combined Wavelet Entropy feature extraction methodology gives good classification accuracy in discriminating the fear-type emotion. The classification accuracy was also enhanced by performing an optimized-SVM kernel. The highest classification accuracy is obtained with a combination of optimised features obtained from WPT with symlet-7 wavelet basis function and Wavelet entropy having coiflet-4 basis function, and optimised SVM up to 90.1%. The algorithms developed in this paper can be further expanded and hybridised into various biological signals, i.e. electromyogram, electrooculogram, MEG, and EKG, for implementing a more unified and versatile human-computer interface. However, we should focus on widening the database by experimenting with subjects for building a robust fear-type emotion detection system using the proposed methodology.

CONFLICT OF INTEREST

The author declares that he has no known competing financial interests or personal relationships that could have appeared to influence the work reported in this paper.

AUTHOR CONTRIBUTION

Çaglar Uyulan: Methodology, Formal analysis, Writing - original draft, Writing - review & editing. **Ahmet Ergun Gümüş**: Data curation, Formal analysis, visualisation. **Zozan Guleken**: Conceptualisation, Methodology, Writing - original draft, Writing - review & editing, Supervision.

REFERENCES

1. E. Osuna, L. F. Rodríguez, J. O. Gutierrez-Garcia, and L. A. Castro, "Development of computational models of emotions: A software engineering perspective," Cogn. Syst. Res., vol. 60, 2020, doi: 10.1016/j.cogsys.2019.11.001.
2. A. Hassouneh, A. M. Mutawa, and M. Murugappan, "Development of a Real-Time Emotion Recognition System Using Facial Expressions and EEG based on machine learning and deep neural network methods," Informatics Med. Unlocked, vol. 20, p. 100372, 2020, doi: 10.1016/j.imu.2020.100372.
3. F. Balducci, C. Grana, and R. Cucchiara, "Affective level design for a role-playing videogame evaluated by a brain–computer interface and machine learning methods," Vis. Comput., vol. 33, no. 4, 2017, doi: 10.1007/s00371-016-1320-2.
4. N. S. Suhaimi, J. Mountstephens, and J. Teo, "EEG-Based Emotion Recognition: A State-of-the-Art Review of Current Trends and Opportunities," Computational Intelligence and Neuroscience, vol. 2020. 2020, doi: 10.1155/2020/8875426.
5. A. Mert and A. Akan, "Emotion recognition from EEG signals by using multivariate empirical mode decomposition," Pattern Anal. Appl., vol. 21, no. 1, 2018, doi: 10.1007/s10044-016-0567-6.
6. M. M. Bradley and P. J. Lang, "Measuring emotion: The self-assessment manikin and the semantic differential," J. Behav. Ther. Exp. Psychiatry, vol. 25, no. 1, 1994, doi: 10.1016/0005-7916(94)90063-9.
7. J. D. Morris, "OBSERVATIONS: SAM: The Self-Assessment Manikin - An Efficient Cross-Cultural Measurement of Emotional Response," J. Advert. Res., vol. 35, no. 6, pp. 63–68, 1995.
8. C. E. Izard, "Emotion theory and research: Highlights, unanswered questions, and emerging issues," Annu. Rev. Psychol., vol. 60, pp. 1–25, 2009, doi: 10.1146/annurev.psych.60.110707.163539.
9. G. Di Flumeri, P. Aricò, G. Borghini, N. Sciaraffa, A. Di Florio, and F. Babiloni, "The dry revolution: Evaluation of three different eeg dry electrode types in terms of signal spectral features, mental states classification and usability," Sensors (Switzerland), vol. 19, no. 6, 2019, doi: 10.3390/s19061365.
10. S. Jeon, J. Chien, C. Song, and J. Hong, "A Preliminary Study on Precision Image Guidance for Electrode Placement in an EEG Study," Brain Topogr., vol. 31, no. 2, 2018, doi: 10.1007/s10548-017-0610-y.
11. J. Fan, J. W. Wade, A. P. Key, Z. E. Warren, and N. Sarkar, "EEG-based affect and workload recognition in a virtual driving environment for ASD intervention," IEEE Trans. Biomed. Eng., vol. 65, no. 1, 2018, doi: 10.1109/TBME.2017.2693157.
12. A. D. Bigirimana, N. Siddique, and D. Coyle, "A hybrid ICA-wavelet transform for automated artefact removal in EEG-based emotion recognition," 2017, doi: 10.1109/SMC.2016.7844928.
13. A. Tandle, N. Jog, P. D'cunha, and M. Chheta, "Classification of Artefacts in EEG Signal Recordings and EOG Artefact Removal using EOG Subtraction," Commun. Appl. Electron., vol. 4, no. 1, 2016, doi: 10.5120/cae2016651997.
14. M. Murugappan and S. Murugappan, "Human emotion recognition through short time Electroencephalogram (EEG) signals using Fast Fourier Transform (FFT)," 2013, doi: 10.1109/CSPA.2013.6530058.
15. M. Horvat, M. Dobrinic, M. Novosel, and P. Jercic, "Assessing emotional responses induced in virtual reality using a consumer EEG headset: A preliminary report," 2018, doi: 10.23919/MIPRO.2018.8400184.
16. Y. Liu et al., "Multi-channel EEG-based emotion recognition via a multi-level features guided capsule network," Comput. Biol. Med., vol. 123, 2020, doi: 10.1016/j.compbiomed.2020.103927.
17. K. Schaaff and T. Schultz, "Towards emotion recognition from electroencephalographic signals," 2009, doi: 10.1109/ACII.2009.5349316.

18. T. T. Erguzel et al., “Entropy: A Promising EEG Biomarker Dichotomizing Subjects With Opioid Use Disorder and Healthy Controls,” Clin. EEG Neurosci., vol. 51, no. 6, 2020, doi: 10.1177/1550059420905724.
19. M. A. Asghar, M. J. Khan, M. Rizwan, M. Shorfuzzaman, and R. M. Mehmood, “AI inspired EEG-based spatial feature selection method using multivariate empirical mode decomposition for emotion classification,” in Multimedia Systems, 2022, vol. 28, no. 4, doi: 10.1007/s00530-021-00782-w.
20. M. Z. I. Ahmed, N. Sinha, S. Phadikar, and E. Ghaderpour, “Automated Feature Extraction on AsMap for Emotion Classification Using EEG,” Sensors, vol. 22, no. 6, 2022, doi: 10.3390/s22062346.
21. X. Zhu et al., “EEG Emotion Classification Network Based on Attention Fusion of Multi-Channel Band Features,” Sensors, vol. 22, no. 14, 2022, doi: 10.3390/s22145252.
22. A. Anuragi, D. Singh Sisodia, and R. Bilas Pachori, “EEG-based cross-subject emotion recognition using Fourier-Bessel series expansion based empirical wavelet transform and NCA feature selection method,” Inf. Sci. (Ny)., vol. 610, pp. 508–524, 2022, doi: 10.1016/j.ins.2022.07.121.
23. C. C. N. Network, J. Dai, X. Xi, G. Li, and T. Wang, “brain sciences EEG-Based Emotion Classification Using Improved,” 2022.
24. Q. Gao, Y. Yang, Q. Kang, Z. Tian, and Y. Song, “EEG-based Emotion Recognition with Feature Fusion Networks,” Int. J. Mach. Learn. Cybern., vol. 13, no. 2, 2022, doi: 10.1007/s13042-021-01414-5.
25. W. Kan, Y. Li, , and , “Emotion recognition from EEG signals by using LSTM recurrent neural networks,” J. Nanjing Univ. Nat. Sci., vol. 55, no. 1, pp. 110–116, 2019.
26. V. Padhmashree and A. Bhattacharyya, “Human emotion recognition based on time–frequency analysis of multivariate EEG signal,” Knowledge-Based Syst., vol. 238, 2022, doi: 10.1016/j.knosys.2021.107867.
27. H. Liu, J. Zhang, Q. Liu, and J. Cao, “Minimum spanning tree based graph neural network for emotion classification using EEG,” Neural Networks, vol. 145, 2022, doi: 10.1016/j.neunet.2021.10.023.
28. P. J. Lang, M. M. Bradley, and B. N. Cuthbert, “International affective picture system (IAPS): Technical manual and affective ratings,” NIMH Cent. Study Emot. Atten., pp. 39–58, 1997.
29. N. Kumar, K. Khaund, and S. M. Hazarika, “Bispectral Analysis of EEG for Emotion Recognition,” Procedia Comput. Sci., vol. 84, pp. 31–35, 2016, doi: 10.1016/j.procs.2016.04.062.
30. R. Yuvaraj et al., “Detection of emotions in Parkinson’s disease using higher order spectral features from brain’s electrical activity,” Biomed. Signal Process. Control, vol. 14, no. 1, pp. 108–116, 2014, doi: 10.1016/j.bspc.2014.07.005.
31. N. A. Badcock, P. Mousikou, Y. Mahajan, P. De Lissa, J. Thie, and G. McArthur, “Validation of the Emotiv EPOC® EEG gaming systemfor measuring research quality auditory ERPs,” PeerJ, vol. 2013, no. 1, pp. 1–17, 2013, doi: 10.7717/peerj.38.
32. M. Klug and K. Gramann, “Identifying key factors for improving ICA-based decomposition of EEG data in mobile and stationary experiments,” Eur. J. Neurosci., no. May, pp. 1–15, 2020, doi: 10.1111/ejn.14992.
33. G. Strang and T. Nguyen, Wavelets and filter banks. Wellesley, MA: Cambridge Press, 1997.
34. A. N. Akansu and R. A. Haddad, Multiresolution Signal Decomposition: Transforms, Subbands, and Wavelets. 2001.
35. J. Gomes and L. Velho, “The Fast Wavelet Transform,” in From Fourier Analysis to Wavelets, 2015.
36. A. Abbate, C. M. DeCusatis, and P. K. Das, “Discrete Wavelet Transform: From Frames to Fast Wavelet Transform,” in Wavelets and Subbands, 2002.
37. H. Heidari Bafroui and A. Ohadi, “Application of wavelet energy and Shannon entropy for feature extraction in gearbox fault detection under varying speed conditions,” Neurocomputing, vol. 133, 2014, doi: 10.1016/j.neucom.2013.12.018.
38. O. A. Rosso et al., “Wavelet entropy: A new tool for analysis of short duration brain electrical signals,” J. Neurosci. Methods, vol. 105, no. 1, 2001, doi: 10.1016/S0165-0270(00)00356-3.
39. F. Salo, A. B. Nassif, and A. Essex, “Dimensionality reduction with IG-PCA and ensemble classifier for network intrusion detection,” Comput. Networks, vol. 148, 2019, doi: 10.1016/j.comnet.2018.11.010.
40. C. Uyulan and T. T. Erguzel, “Analysis of Time – Frequency EEG Feature Extraction Methods for Mental Task Classification,” Int. J. Comput. Intell. Syst., vol. 10, no. 1, 2017, doi: 10.2991/ijcis.10.1.87.
41. C. Uyulan, T. T. Ergüzel, and N. Tarhan, “Entropy-based feature extraction technique in conjunction with wavelet packet transform for multi-mental task classification,” Biomed. Tech., 2019, doi: 10.1515/bmt-2018-0105.
42. R. N. Khushaba, A. Al-Jumaily, and A. Al-Ani, “Novel feature extraction method based on fuzzy entropy and wavelet packet transform for myoelectric control,” 2007, doi: 10.1109/ISCIT.2007.4392044.
43. R. N. Khushaba, S. Kodagoda, S. Lal, and G. Dissanayake, “Driver drowsiness classification using fuzzy wavelet-packet-based feature-extraction algorithm,” IEEE Trans. Biomed. Eng., vol. 58, no. 1, 2011, doi: 10.1109/TBME.2010.2077291.
44. C. Uyulan and T. Erguzel, “Comparison of Wavelet Families for Mental Task Classification,” J. Neurobehav. Sci., vol. 3, no. 2, 2016, doi: 10.5455/jnbs.1454666348.
45. G. I. Webb and Z. Zheng, “Multistrategy ensemble learning: Reducing error by combining ensemble learning techniques,” IEEE Trans. Knowl. Data Eng., vol. 16, no. 8, 2004, doi: 10.1109/TKDE.2004.29.
46. M. Majnik and Z. Bosnić, “ROC analysis of classifiers in machine learning: A survey,” Intelligent Data Analysis, vol. 17, no. 3. 2013, doi: 10.3233/IDA-130592.
47. D. J. Hand, “Measuring classifier performance: A coherent alternative to the area under the ROC curve,” Mach. Learn., vol. 77, no. 1, 2009, doi: 10.1007/s10994-009-5119-5.
48. M. Hamada, B. B. Zaidan, and A. A. Zaidan, “A Systematic Review for Human EEG Brain Signals Based Emotion Classification, Feature Extraction, Brain Condition, Group Comparison,” Journal of Medical Systems, vol. 42, no. 9. 2018, doi: 10.1007/s10916-018-1020-8.
49. K. Guo, H. Candra, H. Yu, H. Li, H. T. Nguyen, and S. W. Su, “EEG-based emotion classification using innovative features and combined SVM and HMM classifier,” 2017, doi: 10.1109/EMBC.2017.8036868.
50. R. Dhiman, Priyanka, and J. S. Saini, “Wavelet analysis of electrical signals from brain: The electroencephalogram,” in Lecture Notes of the Institute for Computer Sciences, Social-Informatics and Telecommunications Engineering, LNICST, 2013, vol. 115, doi: 10.1007/978-3-642-37949-9_24.
51. Z. Mohammadi, J. Frounchi, and M. Amiri, “Wavelet-based emotion recognition system using EEG signal,” Neural Comput. Appl., vol. 28, no. 8, 2017, doi: 10.1007/s00521-015-2149-8.
52. A. Q.-X. Ang, Y. Q. Yeong, and W. Wee, “Emotion Classification from EEG Signals Using Time-Frequency-DWT Features and ANN,” J. Comput. Commun., vol. 05, no. 03, 2017, doi: 10.4236/jcc.2017.53009.
53. R. E. J. Yohanes, W. Ser, and G. Bin Huang, “Discrete Wavelet Transform coefficients for emotion recognition from EEG signals,”

2012, doi: 10.1109/EMBC.2012.6346410.
54. H. Candra, M. Yuwono, R. Chai, H. T. Nguyen, and S. Su, "EEG emotion recognition using reduced channel wavelet entropy and average wavelet coefficient features with normal Mutual Information method," 2017, doi: 10.1109/EMBC.2017.8036862.
55. N. D. Mai, B. G. Lee, and W. Y. Chung, "Affective computing on machine learning-based emotion recognition using a self-made eeg device," Sensors, vol. 21, no. 15, 2021, doi: 10.3390/s21155135.
56. K. Luangrat, Y. Punsawad, and Y. Wongsawat, "On the development of EEG based emotion classification," 2012, doi: 10.1109/BMEiCon.2012.6465506.
57. X. W. Wang, D. Nie, and B. L. Lu, "EEG-based emotion recognition using frequency domain features and support vector machines," in Lecture Notes in Computer Science (including subseries Lecture Notes in Artificial Intelligence and Lecture Notes in Bioinformatics), 2011, vol. 7062 LNCS, no. PART 1, doi: 10.1007/978-3-642-24955-6_87.
58. V. Bajaj and R. B. Pachori, "Human emotion classification from eeg signals using multiwavelet transform," 2014, doi: 10.1109/ICMB.2014.29.
59. A. E. Vijayan, D. Sen, and A. P. Sudheer, "EEG-based emotion recognition using statistical measures and auto-regressive modeling," 2015, doi: 10.1109/CICT.2015.24.
60. S. Alhagry, A. Aly, and R. A., "Emotion Recognition based on EEG using LSTM Recurrent Neural Network," Int. J. Adv. Comput. Sci. Appl., vol. 8, no. 10, 2017, doi: 10.14569/ijacsa.2017.081046.
61. N. Y. Oktavia, A. D. Wibawa, E. S. Pane, and M. H. Purnomo, "Human Emotion Classification Based on EEG Signals Using Naïve Bayes Method," 2019, doi: 10.1109/ISEMANTIC.2019.8884224.
62. J. X. Chen, D. M. Jiang, and Y. N. Zhang, "A Hierarchical Bidirectional GRU Model with Attention for EEG-Based Emotion Classification," IEEE Access, vol. 7, 2019, doi: 10.1109/ACCESS.2019.2936817.
63. Y. P. Lin and T. P. Jung, "Improving EEG-based emotion classification using conditional transfer learning," Front. Hum. Neurosci., vol. 11, 2017, doi: 10.3389/fnhum.2017.00334.
64. J. Atkinson and D. Campos, "Improving BCI-based emotion recognition by combining EEG feature selection and kernel classifiers," Expert Syst. Appl., vol. 47, 2016, doi: 10.1016/j.eswa.2015.10.049.
65. S. E. Moon, S. Jang, and J. S. Lee, "Convolutional Neural Network Approach for EEG-Based Emotion Recognition Using Brain Connectivity and its Spatial Information," in ICASSP, IEEE International Conference on Acoustics, Speech and Signal Processing - Proceedings, 2018, vol. 2018-April, doi: 10.1109/ICASSP.2018.8461315.
66. H. Mei and X. Xu, "EEG-based emotion classification using convolutional neural network," in 2017 International Conference on Security, Pattern Analysis, and Cybernetics, SPAC 2017, 2018, vol. 2018-January, doi: 10.1109/SPAC.2017.8304263.
67. R. M. Mehmood and H. J. Lee, "Emotion classification of EEG brain signal using SVM and KNN," 2015, doi: 10.1109/ICMEW.2015.7169786.
68. B. Kaur, D. Singh, and P. P. Roy, "EEG Based Emotion Classification Mechanism in BCI," Procedia Comput. Sci., vol. 132, no. Iccids, pp. 752–758, 2018, doi: 10.1016/j.procs.2018.05.087.
69. A. Bhardwaj, A. Gupta, P. Jain, A. Rani, and J. Yadav, "Classification of human emotions from EEG signals using SVM and LDA Classifiers," 2015, doi: 10.1109/SPIN.2015.7095376.
70. T. Chen, S. Ju, F. Ren, M. Fan, and Y. Gu, "EEG emotion recognition model based on the LIBSVM classifier," Meas. J. Int. Meas. Confed., vol. 164, 2020, doi: 10.1016/j.measurement.2020.108047.